

# Fractional multiwavelet methods for solving spatiotemporal fractional diffusion equations with non-smooth solutions

Jian Zhang<sup>a</sup> , Chaoyue Guan<sup>b</sup>  and Hong Du<sup>a</sup>  

<sup>a</sup> *College of Mathematics and Computer Science, GuangDong Ocean University, ZhanJiang, Guangdong, China*

<sup>b</sup> *School of Mathematical Sciences, Harbin Normal University, Harbin, Heilongjiang, China*

## Article History:

- received November 11, 2024
- revised February 17, 2025
- accepted February 28, 2025

**Abstract.** This introduces a new method that effectively solves spatiotemporal fractional diffusion equation (FDE) using fractional Lagrange interpolation and fractional multiwavelets. The method effectively addresses situations with non-smooth solutions. The approach begins by discretizing the time variable  $t$  using the fractional piecewise parabolic Lagrange interpolation method. For the spatial variables, we construct fractional multiwavelets. Through the least residue method, we obtain approximate solutions, while also conducting convergence analysis. Numerical demonstrations validate the high accuracy achieved by the proposed method, notably showcasing the better approximation capability of fractional polynomials compared to their integer counterparts.

**Keywords:** fractional calculus; fractional diffusion equation; least residue method; fractional multiwavelets.

**AMS Subject Classification:** 35R11; 65T60.

 Corresponding author. E-mail: [du-hong163@163.com](mailto:du-hong163@163.com)

## 1 Introduction

Fractional calculus has garnered significant attention for its capability to elucidate hereditary properties and memory phenomena across diverse scientific and engineering disciplines. These encompass engineering vibrations [20], viscoelastic mechanics, and rheology [32], control theory [23], and anomalous diffusion [15]. Investigating initial and boundary value problems for the FDE is crucial. Numerous studies highlight its importance, including references [2,4,5]. Importantly, seminal works such as [15] provided demonstrations of stability and the existence of solutions for fractional differential equations. The establishment of the boundedness theorem for general fractional integrals was documented in [11]. Many scholars have explored time fractional partial differential

Copyright © 2025 The Author(s). Published by Vilnius Gediminas Technical University

This is an Open Access article distributed under the terms of the Creative Commons Attribution License (<https://creativecommons.org/licenses/by/4.0/>), which permits unrestricted use, distribution, and reproduction in any medium, provided the original author and source are credited.

equations and have proposed various methods, including the finite difference method [21, 22, 31], spline configuration method [27], Adomian's decomposition method [14], and the local discontinuous Galerkin method [7], among others.

However, as research progresses, many scholars have recognized the need to study fractional derivatives of spatiotemporal variables in the description of various natural phenomena, such as reservoir simulation, fluid flow in porous media, and global water production [24]. The spatiotemporal FDE is used to investigate anomalous diffusion phenomena, including pollutant propagation, heat conduction, and mass transfer. Additionally, it is applied in environmental fluid dynamics to simulate the penetration curve of solute migration, with the aim of providing a more precise description of flow behavior in natural environments [30]. Several authors have proposed various solutions for spatiotemporal fractional equations, such as the homotopy analysis method [25], Adomian decomposition method [16], finite element method [12], Laplace transform homotopy perturbation method [24], and Chebyshev collocation method [10].

Currently, there is limited research on numerical methods for spatiotemporal fractional partial differential equations. The homotopy perturbation transform method, Laplace transform homotopy perturbation method, and Adomian decomposition method have the following limitations: convergence depends on the choice of initial approximation and the number of iterations; furthermore, these methods require high accuracy in approximation and numerical stability.

Recently, many researchers have explored spatiotemporal fractional equations. The method proposed by Kumar et al. [17] provides an efficient and user-friendly approach for solving time-space fractional partial differential equations using Picard's iterative method, showcasing its versatility and simplicity over more complex methods. In [18], the authors present a novel computational technique for solving space-time fractional-order partial differential equations using Caputo-type derivatives. This method is based on operational and pseudo-operational matrices of fractional-order Lagrange polynomials, coupled with Newton's iterative method to solve the resulting algebraic system. In [26], a novel spatio-temporal meshless method is proposed for solving time fractional partial differential equations with variable coefficients, using a multiquadric function and space-time scale framework. This approach avoids fractional derivative approximations and efficiently handles irregular geometries. In [1], a generalized nonlinear fractional integro-reaction-diffusion equation with spatiotemporal variable-order derivatives is introduced. An efficient spectral shifted Legendre tau method is developed to solve the model, addressing challenges from nonlinear terms and SVO functions. Numerical results demonstrate its accuracy and non-local properties. In [13], a pseudospectral method using Chebyshev polynomials is proposed for solving the space-time variable-order fractional diffusion equation with a variable diffusion coefficient. The method provides error bounds and convergence analysis, demonstrating its efficacy and reliability through illustrative examples with various boundary conditions. To the best of our knowledge, published studies have not yet addressed non-smooth solutions.

In this paper, we focus on the spatiotemporal fractional differential equation (FDE) in the Caputo sense to specifically address the challenge of non-smooth

solutions. This model is related to the space-time fractional bioheat equation [28, 29], and the equation of interest is formulated as follows:

$$D_t^\beta u(x, t) = cD_x^\alpha u(x, t) + s(x, t), \quad 0 < x < 1, \quad t > 0, \quad (1.1)$$

where  $0 < \beta \leq 1$ ,  $1 < \alpha \leq 2$ ,  $c$  is a constant, and  $s(x, t)$  represents a source term, subject to the initial and Dirichlet boundary conditions:

$$\begin{aligned} u(x, 0) &= u_0(x), \quad 0 < x < 1, \\ u(0, t) &= b_0(t), \quad u(1, t) = b_1(t), \quad t > 0. \end{aligned}$$

Currently, there are several gaps and challenges in the numerical solution of spatiotemporal fractional differential equations:

- Existing methods such as the Chebyshev collocation method [10] face stability issues, involve complex node selection, and struggle with boundary condition handling, making it difficult to provide sufficiently localized solutions.
- The finite element method [12] effectively solves the initial-boundary value problem, but there are still limitations in terms of accuracy, computational cost, and sensitivity to mesh quality.

To address these gaps, this paper proposes an innovative approach:

- The time fractional derivative term is approximated using a fractional piecewise parabolic interpolation method, overcoming stability and computational complexity issues in traditional methods.
- A fractional multiscale wavelet basis is employed to approximate the spatial variables, exploiting its high precision and locality, significantly improving accuracy.
- Numerical results show that when an appropriate polynomial degree is chosen, the proposed method achieves higher accuracy and overcomes the limitations found in traditional methods.

The main structure of this paper can be outlined as follows: Section 2 sets the foundational theoretical frameworks of multiwavelets bases. In Section 3, after discretizing the time variable, the matrix equation associated with the spatial variable is delineated. Afterward, in Section 4, we employ the method of least residue method to derive an approximate solution for Equation (1.1), and we also present a theorem regarding the convergence order. Section 5 demonstrates various experiments, and provide a simple summary in Section 6.

## 2 Multiwavelet bases

Multiwavelets bases are local bases that support intervals approaching zero and are orthogonal in  $L^2[0, 1]$ .

The two-scale relations for Legendre scaling functions of 3-order, are in the form [3]:

$$\phi^i(a) = \sum_{j=0}^3 q_{ij} \xi^j(2a) + \sum_{j=0}^3 q_{i,r+j+1} \xi^j(2a-1), \quad (2.1)$$

where  $q_{ij}$  are unknown coefficients. The cubic Legendre scaling functions  $\xi^j(a)$  ( $j = 0, 1, 2, 3$ ) consisting of four functions are the following [19]:

$$\begin{aligned} \xi^0(a) &= 1, \quad a \in [0, 1], & \xi^1(a) &= \sqrt{3}(2a-1), \quad a \in [0, 1], \\ \xi^2(a) &= \sqrt{5}(6a^2-6a-1), \quad a \in [0, 1], \\ \xi^3(a) &= \sqrt{7}(20a^3-30a^2+12a-1), \quad a \in [0, 1]. \end{aligned}$$

By replacing the independent variable  $a$  in Equation (2.1) with  $b^\lambda$ , the Equation (2.1) can be rewritten as follows:

$$\phi^i(b) = \sum_{j=0}^r q_{ij} \xi^j(2b^\lambda) + \sum_{j=0}^r q_{i,r+j+1} \xi^j(2b^\lambda-1). \quad (2.2)$$

According to the vanishing moment and orthogonality of multiwavelets in [3], the following lemma can be obtained.

**Lemma 1.** *Multiwavelets (2.2) satisfy properties of vanishing moments*

$$\int_0^1 \omega(b) \phi^i(b) (b^\lambda)^j db = 0, \quad i = 0, 1, \dots, r, \quad j = 0, 1, \dots, i+r \quad (2.3)$$

and orthonormality

$$\int_0^1 \omega(b) \phi^i(b) \phi^j(b) db = \delta_{ij}, \quad i, j = 0, 1, \dots, r, \quad (2.4)$$

where  $\delta_{ij} = \begin{cases} 1, & i = j \\ 0, & i \neq j \end{cases}$ , and weight function  $\omega(b) = \lambda b^{\lambda-1}$ .

By conditions (2.3) and (2.4), the fractional Legendre wavelets are constructed.

$$\begin{aligned} \phi_{10}^0(b) &= \begin{cases} h_{01}(b) = \sqrt{\frac{15}{17}} (224b^{3\lambda} - 216b^{2\lambda} + 56b^\lambda - 3), & b \in [0, (1/2)^{\frac{1}{\lambda}}), \\ h_{02}(b) = \sqrt{\frac{15}{17}} (-224b^{3\lambda} + 456b^{2\lambda} - 296b^\lambda + 61), & b \in [(1/2)^{\frac{1}{\lambda}}, 1], \end{cases} \\ \phi_{10}^1(b) &= \begin{cases} h_{11}(b) = \sqrt{\frac{1}{21}} (1680b^{3\lambda} - 1320b^{2\lambda} + 270b^\lambda - 11), & b \in [0, (1/2)^{\frac{1}{\lambda}}), \\ h_{12}(b) = \sqrt{\frac{1}{21}} (1680b^{3\lambda} - 3720b^{2\lambda} + 2670b^\lambda - 619), & b \in [(1/2)^{\frac{1}{\lambda}}, 1], \end{cases} \\ \phi_{10}^2(b) &= \begin{cases} h_{21}(b) = \sqrt{\frac{35}{17}} (256b^{3\lambda} - 174b^{2\lambda} + 30b^\lambda - 1), & b \in [0, (1/2)^{\frac{1}{\lambda}}), \\ h_{22}(b) = \sqrt{\frac{35}{17}} (-256b^{3\lambda} + 594b^{2\lambda} - 450b^\lambda + 111), & b \in [(1/2)^{\frac{1}{\lambda}}, 1], \end{cases} \\ \phi_{10}^3(b) &= \begin{cases} h_{31}(b) = \sqrt{\frac{5}{21}} (-420b^{3\lambda} + 246b^{2\lambda} - 36b^\lambda + 1), & b \in [0, (1/2)^{\frac{1}{\lambda}}), \\ h_{32}(b) = \sqrt{\frac{5}{21}} (-420b^{3\lambda} + 1014b^{2\lambda} - 804b^\lambda + 209), & b \in [(1/2)^{\frac{1}{\lambda}}, 1], \end{cases} \end{aligned}$$

So the multiwavelets are written as

$$\begin{aligned} \phi_{ik}^m(b) &= 2^{\frac{i-1}{2}} \phi_{10}^m \left( (2^{i-1}b^\lambda - k)^{\frac{1}{\lambda}} \right) \\ &= \begin{cases} 2^{\frac{i-1}{2}} h_{m1} \left( (2^{i-1}b^\lambda - k)^{\frac{1}{\lambda}} \right), & b \in \left[ \left( \frac{k}{2^{i-1}} \right)^{\frac{1}{\lambda}}, \left( \frac{k+1/2}{2^{i-1}} \right)^{\frac{1}{\lambda}} \right], \\ 2^{\frac{i-1}{2}} h_{m2} \left( (2^{i-1}b^\lambda - k)^{\frac{1}{\lambda}} \right), & b \in \left[ \left( \frac{k+1/2}{2^{i-1}} \right)^{\frac{1}{\lambda}}, \left( \frac{k+1}{2^{i-1}} \right)^{\frac{1}{\lambda}} \right], \\ 0, & \text{else,} \end{cases} \end{aligned}$$

where  $m = 0, 1, 2, 3, i = 2, 3, \dots, k = 0, 1, \dots, 2^{i-1} - 1$ . For simplicity, this rearrangement is permitted

$$\begin{aligned} \{\psi_j(b)\}_{j=0}^\infty &= \left\{ \xi^m(b), \phi_{ik}^m(b), m = 0, 1, 2, 3, i = 1, 2, \dots, k = 0, 1, \dots, 2^{i-1} - 1 \right\} \\ &= \left\{ \xi^0, \xi^1, \xi^2, \xi^3, \phi_{10}^0, \phi_{10}^1, \phi_{10}^2, \phi_{10}^3, \phi_{20}^0, \phi_{20}^1, \phi_{20}^2, \phi_{20}^3, \phi_{30}^0, \dots \right\}. \end{aligned}$$

Similar to Lemma 3.2 in [9], we can obtain the following lemma.

- Lemma 2.** (1)  $\{\psi_j(b)\}_{j=0}^\infty$  is a set of multiscale orthonormal bases with weight function  $\omega(b) = \lambda b^{\lambda-1}$  in  $L^2[0, 1]$ .  
 (2)  $\{\phi_{10}^m(b), m = 0, 1, 2, 3\}$  have  $m + 4$  order vanishing moments.

### 3 Discretization

#### 3.1 Discretization time variable $t$

The fractional piecewise parabolic Lagrange interpolation method is now applied to discretize the time variable  $t$ . We partition  $[0, T]$  into  $2N$  segments  $\{t_q = qh_1, 0 \leq q \leq 2N\}$  with a step size of  $h_1 = \frac{T}{2N}$ . The initial condition  $u(x, 0) = u_0(x)$  in Equation (1.1) is replaced by the nodes  $t_q$

$$D_t^\beta u(x, t_q) = cD_x^\alpha u(x, t_q) + s(x, t_q). \tag{3.1}$$

Utilizing definition of Caputo derivative, it has

$$D_t^\beta u(x, t_q) = \frac{1}{\Gamma(1 - \beta)} \int_0^{t_q} \frac{\partial u(x, \tau)}{\partial \tau} (t_q - \tau)^{-\beta} d\tau. \tag{3.2}$$

On the interval  $[t_{2(p-1)}, t_{2p}]$ ,  $1 \leq p \leq N$ , the fractional piecewise parabolic Lagrange interpolation functions  $P_p(x, t)$  and their first-order derivative functions satisfy

$$\begin{aligned} P_p(x, t) &= \sum_{j=2(p-1)}^{2p} u(x, t_j) \prod_{j=2(p-1), m \neq j}^{2p} \frac{t^\nu - t_j^\nu}{t_m^\nu - t_j^\nu}, \\ \frac{\partial u(x, t)}{\partial t} &\simeq \frac{\partial P_p(x, t)}{\partial t} = \sum_{j=2(p-1)}^{2p} u(x, t_j) \frac{d \left( \prod_{j=2(p-1), m \neq j}^{2p} \frac{t^\nu - t_j^\nu}{t_m^\nu - t_j^\nu} \right)}{dt}. \end{aligned} \tag{3.3}$$

By substituting (3.3) into (3.2) and defining  $\{H_{k,q}, q = 2p - 1, 2p\}_{p=1}^N$  as the coefficients of  $u(x, t_k)$ , we obtain

$$\begin{aligned} & \sum_{k=0}^{2p} u(x, t_k) H_{k,q} \triangleq D_t^\beta u(x, t_q) \\ & \simeq \frac{1}{\Gamma(1-\beta)} \left( \sum_{i=1}^{p-1} \int_{2(i-1)h}^{2ih} \frac{\partial P_i(x, \tau)}{\partial \tau} + \int_{2(p-1)h}^{qh} \frac{\partial P_p(x, \tau)}{\partial \tau} \right) (t_q - \tau)^{-\beta} d\tau. \end{aligned} \tag{3.4}$$

On every subinterval  $[t_{2(p-1)}, t_{2p}]$ , substituting (3.4) into (3.1),  $u(x, t_q)$  can be solved by

$$\sum_{k=2p-1}^{2p} u(x, t_k) H_{k,q} - cD_x^\alpha u(x, t_q) = - \sum_{k=0}^{2(p-1)} u(x, t_k) H_{k,q} + s(x, t_q).$$

On  $[t_{2(p-1)}, t_{2p}]$ ,  $p = 1, \dots, N$ , define

$$\mathbf{U}_p(x) = (u(x, t_{2p-1}), u(x, t_{2p}))^T, \quad \mathbf{F}_p(x) = (f(x, t_{2p-1}), f(x, t_{2p}))^T,$$

where  $f(x, t_q) = - \sum_{k=0}^{2(p-1)} u(x, t_k) H_{k,q} + s(x, t_q)$ ,  $q = 2p - 1, 2p$ .

Let  $u'(x) \in C[0, 1]$ . To improve regularity, we perform a smooth transformation such that  $x = s^{\frac{1}{\gamma}}$ . At this point,  $\tilde{u}'_x(s) \triangleq u'_x(s^{\frac{1}{\gamma}}) \in C^1[a, b]$ . Denote the Banach space

$$S = \{u(x) \mid u'(x) \in C[0, 1], \tilde{u}'_x(s) \in C^1[0, 1]\},$$

with the norm defined as

$$\|u(x)\|_S = \|\tilde{u}'_x(s)\|_{C^1[0,1]}.$$

Define  $\mathcal{G}_p = (\mathcal{G}_{p,**})_{2 \times 2} : S \rightarrow C[0, 1]$ , where entries are of the form

$$\begin{cases} \mathcal{G}_{p,11} = H_{2p-1,2p-1} - cD_x^\alpha, & \mathcal{G}_{p,12} = H_{2p,2p-1}, \\ \mathcal{G}_{p,21} = H_{2p-1,2p}, & \mathcal{G}_{p,22} = H_{2p,2p} - cD_x^\alpha. \end{cases}$$

Obtain the following matrix equation

$$\mathcal{G}_p \mathbf{U}_p(x) = \mathbf{F}_p(x), \quad p = 1, \dots, N, \tag{3.5}$$

satisfying the boundary condition  $\mathbf{U}_p(0) = (b_0, b_0)^T$ ,  $\mathbf{U}_p(1) = (b_1, b_1)^T$ .

### 3.2 Bounded linear operator

DEFINITION 1. Let  $u_1, u_2 \in C^k[0, 1]$ ,  $\mathbf{u} = (u_1, u_2)^T \in (C^k[0, 1])^2$ , then  $\|\mathbf{u}\|_{(C^k[0,1])^2}^2 = \|u_1\|_{C^k[0,1]}^2 + \|u_2\|_{C^k[0,1]}^2$ , where  $k \in \mathbb{N}$ .

Lemma 3.  $D_x^\alpha u(x)$  is bounded on  $x \in [0, 1]$ , when  $u(x) \in S$ ,  $\alpha - 1 < \gamma < 1$ .

*Proof.* Record  $u'(x)$  as  $v(x)$ . Because  $u(x) \in S$ ,  $v(x) \in C[0, 1]$ . After smooth transformation  $x = s^{\frac{1}{\gamma}}$ ,  $\tilde{v}(s) \triangleq v(s^{\frac{1}{\gamma}}) \in C^1[0, 1]$ . By the definition of Caputo derivative,  $1 < \alpha < 2$ ,  $M_1$  is a constant, one has

$$\begin{aligned} D_x^\alpha u(x) &= \frac{1}{\Gamma(2-\alpha)} \int_0^x (x-\tau)^{1-\alpha} u''(\tau) d\tau = \frac{1}{\Gamma(2-\alpha)} \int_0^x (x-\tau)^{1-\alpha} v'(\tau) d\tau \\ &\stackrel{\tau=\tau_1^{\frac{1}{\gamma}}}{=} \frac{1}{\Gamma(2-\alpha)} \int_0^{x^\gamma} (x-\tau_1^{\frac{1}{\gamma}})^{1-\alpha} [v(\tau_1^{\frac{1}{\gamma}})]'_\tau \cdot \frac{1}{\gamma} \tau_1^{\frac{1}{\gamma}-1} d\tau_1 \\ &= \frac{1}{\Gamma(2-\alpha)} \int_0^{x^\gamma} (x-\tau_1^{\frac{1}{\gamma}})^{1-\alpha} v'_{\tau_1}(\tau_1^{\frac{1}{\gamma}}) \cdot \gamma \tau_1^{1-\frac{1}{\gamma}} \cdot \frac{1}{\gamma} \tau_1^{\frac{1}{\gamma}-1} d\tau_1 \\ &= \frac{1}{\Gamma(2-\alpha)} \int_0^{x^\gamma} (x-\tau_1^{\frac{1}{\gamma}})^{1-\alpha} \tilde{v}'(\tau_1) d\tau_1 \leq \frac{M_1}{\Gamma(2-\alpha)} \int_0^{x^\gamma} (x-\tau_1^{\frac{1}{\gamma}})^{1-\alpha} d\tau_1 \\ &\stackrel{\tau_1=\tau_2^\gamma}{=} \frac{\gamma M_1}{\Gamma(2-\alpha)} \int_0^x (x-\tau_2)^{1-\alpha} \tau_2^{\gamma-1} d\tau_2 = \frac{\gamma M_1 \Gamma(\gamma)}{\Gamma(2-\alpha+\gamma)} \cdot x^{1-\alpha+\gamma} \\ &\leq \frac{\gamma M_1 \Gamma(\gamma)}{\Gamma(2-\alpha+\gamma)}. \end{aligned}$$

□

*Remark 1.* To consider the existence of  $\gamma$  in Lemma 3, let  $u(x) = x^k$  where  $k \geq \alpha$ . Then,  $v(x) \triangleq u'(x) = kx^{k-1}$ , the  $v$  transformed by  $x = s^{\frac{1}{\gamma}}$  is given by:

$$v(x) = v(s^{\frac{1}{\gamma}}) = k \cdot s^{\frac{k-1}{\gamma}} \in C^1[a, b].$$

From this, it follows that  $\frac{k-1}{\gamma} \geq 1$ , and thus  $\gamma \leq k - 1$ . According to the assumptions of Lemma 3,  $\alpha - 1 < \gamma \leq k - 1$ .

**Lemma 4.**  $\mathcal{G}_{p,ik} : S \rightarrow C[0, 1]$ ,  $i, k = 1, 2$ , are linear and bounded for  $1 \leq p \leq N$ .

*Proof.* This only proves that  $\mathcal{G}_{p,11}$  are linear and bounded. For any  $u(x) \in S$ , there exists  $M_2 > 0$ , such that

$$\begin{aligned} \|\mathcal{G}_{p,11}u(x)\|_{C[0,1]} &= \|H_{2p-1,2p-1}u(x) - cD_x^\alpha u(x)\|_{C[0,1]} \\ &\leq (|H_{2p-1,2p-1}| + |c| \|D_x^\alpha\|) \|u(x)\|_S \leq (|H_{2p-1,2p-1}| + |cM_2|) \|u(x)\|_S. \end{aligned}$$

And other operators can be similarly proven. □

**Lemma 5.**  $\mathcal{G}_p : S^2 \rightarrow (C[0, 1])^2$  are bounded linear operators.

*Proof.* For any  $\mathbf{u}(x) = (u_1(x), u_2(x))^T \in S^2$ , according to Lemma 4, select a constant  $M_3$  such that

$$\|\mathcal{G}_{p,ik}\| \leq M_3, \quad i, k = 1, 2,$$

then,

$$\begin{aligned} \|\mathcal{G}_p \mathbf{u}(x)\|_{(C[0,1])^2}^2 &= \sum_{i=1}^2 \left\| \sum_{k=1}^2 \mathcal{G}_{p,ik} u_k(x) \right\|_{C[0,1]}^2 \leq \sum_{i=1}^2 \sum_{k=1}^2 \|\mathcal{G}_{i,k}\|^2 \|u_k(x)\|_S^2 \\ &\leq M_3^2 \sum_{i=1}^2 \sum_{k=1}^2 \|u_k(x)\|_S^2 = 2M_3^2 \sum_{k=1}^2 \|u_k(x)\|_S^2 = 2M_3^2 \|\mathbf{u}(x)\|_{S^2}^2. \end{aligned}$$

□

## 4 The least residue method

### 4.1 The least residue solution

Next, we use multiwavelets bases to approximate  $u'(x)$ ,

$$u'(x) = \sum_{j=0}^d c_j \psi_j(x), \quad j = 0, 1, \dots, d,$$

where  $c_j$  are constants. The notation  $J_0^k$  denotes the Riemann-Liouville fractional integration operator of order  $k$  [6]. From this, it can be concluded that

$$u(x) = \sum_{j=0}^d c_j J_0^1 \psi_j(x), \quad j = 0, 1, \dots, d,$$

where  $c_j$  are constants. In order to make the format of the formula more concise during our discussion, we use  $\square_*(x)$  to represent  $\square(x, t_*)$ , where  $\square$  represents different functions.

**DEFINITION 2.** For any  $\varepsilon > 0$ , let  $\bar{\mathbf{u}}_p(x) = (\bar{u}_{2p-1}(x), \bar{u}_{2p}(x))^T \in S^2$ , if  $\bar{\mathbf{u}}_p(x)$  satisfied

$$\begin{aligned} &\|\mathcal{G}_p \bar{\mathbf{u}}_p(x) - \mathbf{F}_p(x)\|_{(C[0,1])^2}^2 + \sum_{k_1=0}^1 \sum_{q=2p-1}^{2p} (\bar{u}_q(k_1) - b_{k_1})^2 = \sum_{i_1=1}^2 \\ &\times \left\| \sum_{k=1}^2 (\mathcal{G}_{p,i_1 k} \bar{u}_{2p-2+k}(x) - f_{2p-2+k}(x)) \right\|_{C[0,1]}^2 + \sum_{k_1=0}^1 \sum_{q=2p-1}^{2p} (\bar{u}_q(k_1) - b_{k_1})^2 \leq \varepsilon, \end{aligned}$$

then  $\bar{\mathbf{u}}_p$  are the residue solution of Equation (3.5).

**Theorem 1.** For any  $\varepsilon > 0$ , there exists  $M_4 \in \mathbb{N}$  such that for each positive integer  $n \geq M_4$ , the function

$$u_q^d(x) = \sum_{j=0}^d c_{q,j}^d J_0^1 \psi_j(x)$$

for  $q = 2p - 1, 2p, 1 \leq p \leq N$ , serves as the least residue solution of Equation (3.5) if the coefficients  $c_{q,j}^d$  satisfy

$$\begin{aligned} & \|\mathcal{G}_p \mathbf{u}_p^d(x) - \mathbf{F}_p(x)\|_{C[0,1]}^2 + \sum_{k_1=0}^1 \sum_{q=2p-1}^{2p} (u_q^d(k_1) - b_{k_1})^2 \\ &= \min_{\bar{\mathbf{u}}_p \in S^2} \left( \|\mathcal{G}_p \bar{\mathbf{u}}_p(x) - \mathbf{F}_p(x)\|_{C[0,1]}^2 + \sum_{k_1=0}^1 \sum_{q=2p-1}^{2p} (\bar{u}_q(k_1) - b_{k_1})^2 \right) \leq \varepsilon \end{aligned}$$

where  $\mathbf{u}_p^d(x) = (u_{2p-1}^d(x), u_{2p}^d(x))^T, \bar{\mathbf{u}}_p(x) = (\bar{u}_{2p-1}(x), \bar{u}_{2p}(x))^T$ .

*Proof.* Let  $\mathbf{u}_p(x) = (u_{2p-1}(x), u_{2p}(x))^T$  be the exact solution of Equation (3.5). According to Lemma 4, for any  $\varepsilon > 0$ , there exists  $M_4 \in \mathbb{N}$ , such that for each positive integer  $n \geq M_4$ , the function  $\bar{u}_q(x) = \sum_{j=0}^n c_{q,j} \psi_j(x) \in S, q = 2p - 1, 2p$ , satisfies

$$\begin{aligned} & \|\bar{u}_{2p-2+k}(x) - u_{2p-2+k}(x)\|_S \leq \sqrt{\varepsilon / (8 \max(\|\mathcal{G}_{p,ik}\|^2))}, \quad i, k = 1, 2, \\ & \sum_{k_1=0}^1 \sum_{q=2p-1}^{2p} (\bar{u}_q(k_1) - b_{k_1})^2 \leq \frac{\varepsilon}{2}, \\ & \|\mathcal{G}_p \mathbf{u}_p^d(x) - \mathbf{F}_p(x)\|_{C[0,1]}^2 + \sum_{k_1=0}^1 \sum_{q=2p-1}^{2p} (u_q^d(k_1) - b_{k_1})^2 \\ & \leq \|\mathcal{G}_p \bar{\mathbf{u}}_p(x) - \mathbf{F}_p(x)\|_{C[0,1]}^2 + \sum_{k_1=0}^1 \sum_{q=2p-1}^{2p} (\bar{u}_q(k_1) - b_{k_1})^2 \\ & = \|\mathcal{G}_p \bar{\mathbf{u}}_p(x) - \mathcal{G}_p \mathbf{u}_p(x)\|_{C[0,1]}^2 + \sum_{k_1=0}^1 \sum_{q=2p-1}^{2p} (\bar{u}_q(k_1) - b_{k_1})^2 = \sum_{i=1}^2 \\ & \times \left\| \sum_{k=1}^2 (\mathcal{G}_{p,ik} \bar{u}_{2p-2+k}(x) - \mathcal{G}_{p,ik} u_{2p-2+k}(x)) \right\|_{C[0,1]}^2 + \sum_{k_1=0}^1 \sum_{q=2p-1}^{2p} (\bar{u}_q(k_1) - b_{k_1})^2 \\ & \leq \sum_{i=1}^2 \sum_{k=1}^2 \left( \|\mathcal{G}_{p,ik}\|^2 \|\bar{u}_{2p-2+k}(x) - u_{2p-2+k}(x)\|_{C[0,1]}^2 \right) + \frac{\varepsilon}{2} \leq \frac{\varepsilon}{2} + \frac{\varepsilon}{2} = \varepsilon. \end{aligned}$$

This indicates that  $\mathbf{u}_p^d$  are the least residue solution of Equation (3.5).  $\square$

### 4.2 The approximate solution of Equation (3.5)

**Theorem 2.** If Equation (3.5) is well-posed, then  $\mathbf{u}_p^d (1 \leq p \leq N)$  provided by Theorem 1 are exactly the approximate solution.

*Proof.* Since  $\mathbf{u}_p^d$  are the least residue solutions, for each given  $\varepsilon > 0$ ,

$$\|\mathcal{G}_p \mathbf{u}_p^d(x) - \mathbf{F}_p(x)\|_{C[0,1]}^2 \leq \varepsilon, \quad \sum_{k_1=0}^1 \sum_{q=2p-1}^{2p} (u_q^d(k_1) - b_{k_1})^2 \leq \varepsilon. \quad (4.1)$$

Assume that

$$\mathcal{G}_p \mathbf{u}_p^d(x) = \mathbf{F}_p^d(x), \quad u_q^d(k_1) = b_{k_1}^d, \quad q = 2p - 1, 2p, \quad k_1 = 0, 1,$$

Equations (4.1) yield

$$\|\mathbf{F}_p^d(x) - \mathbf{F}_p(x)\|_{C[0,1]}^2 \leq \varepsilon, \quad \sum_{k_1=0}^1 \sum_{q=2p-1}^{2p} (b_{k_1}^d - b_{k_1})^2 \leq \varepsilon.$$

Since Equation (3.5) is well-posed, for the small enough distribution  $\varepsilon$ , there exists a constant  $M_5$  such that

$$\|\mathbf{u}_p^d(x) - \mathbf{u}_p(x)\|_{S^2} \leq M_5 \varepsilon.$$

It implies that  $\mathbf{u}_p^d(x)$  are the approximate solution of Equation (3.5) on  $[0, 1]$ .  
□

### 4.3 Convergence order

The proof in this subsection is similar to Theorem 2.4 in [8]. Let  $u(x) \in H^3[0, 1]$ , the polynomial function  $u_d(x)$  of degree  $d$  is the projection of  $u(x)$  from  $H^2[0, 1]$  to  $\mathcal{P}_d[0, 1]$ , whenever  $d + 1 \geq 3$ .  $\mathcal{P}_d[0, 1]$  consists of polynomials of order less than or equal to  $d$ . From Equation (28) in the literature [8], it can be derived that

$$\|u(x) - u_d(x)\|_{C^1[0,1]} \leq (1/4)K_1 d^{-1} \|u_{s_1 s_1 s_1}'''(x)\|_{L^2[0,1]},$$

where  $K_1$  is constant,  $s_1 = 2x - 1$ .

**Theorem 3.** Let  $u_q(x)$  and  $u_q^d(x)$  be the exact and approximate solutions of (1.1), respectively, at  $t = t_q$ , for  $q = 2p - 1, 2p$ . Applying  $x^\gamma = s$ , assume that  $[u_q(s^{\frac{1}{\gamma}})]'_x \in H^3[0, 1]$ , when  $\gamma > \alpha - 1$ , show that

$$\|u_q(x) - u_q^d(x)\|_{S[0,1]} \leq K_2 d^{-1} \left\| \left( u_q(s^{\frac{1}{\gamma}}) \right)''''_s \right\|_{L^2[0,1]},$$

where  $K_2$  is constant.

## 5 Numerical examples

In this section, we will provide some examples. Let  $u(x, t)$  be the exact solution and  $u^d(x, t)$  be approximate solutions of Equation (1.1). We define the error metrics as follows:

$$E_2(d) = \max_{1 \leq i \leq 2p} \|u(x, t_i) - u^d(x, t_i)\|_{L^2} = \max_{1 \leq i \leq 2p} \left( \int_0^1 |u(x, t_i) - u^d(x, t_i)|^2 dx \right)^{1/2},$$

$$E_c(d) = \max_{0 \leq x \leq 1} |u(x, t_i) - u^d(x, t_i)|.$$

Here,  $N$  stands for the number of divisions of the interval  $[0, 1]$  into segments, and  $d$  represents the degree of multiwavelets. To obtain the numerical results, we used the software package Mathematica 11.

*Example 1.* Consider the FDE [10]

$$D_t^{\frac{1}{2}} u(x, t) = D_x^{\frac{3}{2}} u(x, t) + s(x, t), \quad 0 < x < 1, \quad t > 0,$$

$$u(x, 0) = x^2(1 - x), \quad u(0, t) = u(1, t) = 0,$$

where  $s(x, t) = \frac{4}{3} \sqrt{\frac{x}{\pi}} \left( 2(1 - x)(tx)^{\frac{3}{2}} + 3(1 + t^2)(2x - 1) \right)$ . The exact solution is  $u(x, t) = x^2(1 - x)(1 + t^2)$ . To provide a comparison with other methods, we present this example. In the Chebyshev collocation method [10], the highest accuracy achieved occurs with a stride of 1/80, resulting in an accuracy of 0.000718710 at  $t = 1$ . In contrast, using the method described in this paper with parameters  $N = 2, d = 4, \gamma = 1,$  and  $\nu = 1,$  the error reaches  $6.92187 \times 10^{-16}$  at  $t = 1,$  approaching the exact solution. Therefore, our method demonstrates significantly higher accuracy compared to the Chebyshev collocation method.

*Example 2.* Consider the FDE [12]

$$D_t^\beta u(x, t) = D_x^\alpha u(x, t) + s(x, t), \quad 0 < x < 1, \quad t > 0,$$

$$u(x, 0) = 0, \quad u(0, t) = 0, \quad u(1, t) = t^2,$$

where the  $s(x, t) = 2t^2 x^2 \left( \frac{t^{-\beta}}{\Gamma(3-\beta)} - \frac{x^{-\alpha}}{\Gamma(3-\alpha)} \right)$ . The exact solution is  $u(x, t) = t^2 x^2$ . We compared our method with the Finite element method in [12], and the numerical results are presented in Table 1. We varied the values of  $\alpha$  and  $\beta,$  and the numerical results indicate that using our method for solving yields higher accuracy under different value selections.

**Table 1.** Comparison of errors under the  $L^2$  norm of Example 2.

	$\alpha = 0.3$	$\alpha = 0.6$	$\alpha = 0.9$	$\beta = 1.3$	$\beta = 1.6$	$\beta = 1.9$
[12]	$(h, \tau) = (\frac{1}{160}, \frac{1}{160^2}), \beta = 1.6$			$(h, \tau) = (\frac{1}{1000}, \frac{1}{32}), \alpha = 0.6$		
GTDS $E_2$	3.6570e-06	3.5749e-06	2.2714e-06	4.3163e-05	2.5396e-04	1.2263e-03
[12]	$(h, \tau) = (\frac{1}{160}, \frac{1}{160}), \beta = 1.6$			$(h, \tau) = (\frac{1}{2000}, \frac{1}{32}), \alpha = 0.6$		
NTDS $E_2$	3.3260E-06	3.4220e-06	2.1922e-06	6.6030E-06	5.0245e-06	1.4870e-06
OUR $E_2(8)$	$(\gamma, \nu) = (\frac{1}{2}, 1), N = 3, \beta = 1.6$			$(\gamma, \nu) = (\frac{1}{2}, 1), N = 3, \alpha = 0.6$		
	3.72747e-17	1.59234e-16	2.13857e-16	1.77076e-15	1.59234e-16	1.19897e-16

*Example 3.* Consider the FDE

$$D_t^{\frac{1}{3}} u(x, t) = D_x^{\frac{3}{2}} u(x, t) + s(x, t), \quad 0 < x < 1, \quad t > 0,$$

$$u(x, 0) = x^{\frac{3}{2}}(1 - x), \quad u(0, t) = u(1, t) = 0,$$

where the  $s(x, t)$  is a corresponding function. The exact solution  $u(x, t) = x^{\frac{3}{2}}(1 - x)(1 + t^{\lambda t})$ . We introduced this example to highlight the contrast between fractional polynomial interpolation and integer polynomial interpolation. Both

fractional polynomials and integer polynomials are employed for discrete time  $t$ , and the numerical results are presented in Table 2 and Figure 1. It is worth noting that when  $\nu = 1$ , the error curves of  $d = 8$  and  $d = 16$  almost overlap in Figure 1, indicating that the accuracy cannot be further improved when  $\nu$  is an integer. The findings suggest that the use of fractional polynomials for discretization yields more satisfactory results.

**Table 2.** Absolute error  $E_c$  of Example 3 ( $N = 5$ ).

	$E_c(4)$	$E_c(8)$	$E_c(16)$	$E_c(8)$
$t$	$(\gamma, \nu) = (\frac{1}{2}, 1), \lambda_t = \frac{5}{6}$			$(\gamma, \nu) = (\frac{1}{2}, \frac{5}{6}), \lambda_t = \frac{5}{6}$
0.1	2.79043e-04	1.34739e-04	1.34795e-04	1.04083e-15
0.2	5.43128e-05	4.80211e-05	4.81118e-05	6.38378e-16
0.3	5.40662e-06	6.68379e-06	6.68844e-06	4.13350e-16
0.4	6.31187e-06	1.13802e-06	1.12830e-06	2.77556e-16
0.5	3.29738e-06	4.64651e-06	4.64532e-06	1.20127e-15
0.6	4.08313e-06	1.59692e-06	1.59321e-06	7.21645e-16
0.7	1.43253e-06	3.01467e-06	3.01371e-06	9.15934e-16
0.8	3.37098e-06	1.45522e-06	1.45307e-06	1.64031e-15
0.9	7.34021e-07	2.16598e-06	2.16520e-06	2.27596e-15
$t$	$(\gamma, \nu) = (\frac{1}{2}, 1), \lambda_t = \frac{2}{3}$			$(\gamma, \nu) = (\frac{1}{2}, \frac{2}{3}), \lambda_t = \frac{2}{3}$
0.1	8.96549e-04	4.55825e-04	4.56016e-04	9.09417e-16
0.2	1.62855e-04	1.39462e-04	1.39754e-04	2.22309e-16
0.3	8.86102e-06	2.23623e-05	2.23727e-05	4.44089e-16
0.4	2.67019e-05	1.02334e-05	1.02020e-05	1.46434e-15
0.5	6.14195e-06	1.59809e-05	1.59751e-05	8.60423e-16
0.6	2.00822e-05	8.52418e-06	8.51393e-06	1.05471e-15
0.7	2.41112e-06	1.04695e-05	1.04653e-05	2.60902e-15
0.8	1.52178e-05	6.76232e-06	6.75620e-06	1.99840e-15
0.9	1.88089e-06	7.57367e-06	7.57045e-06	2.49800e-15

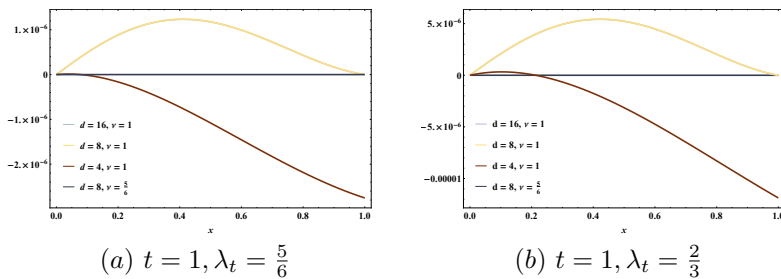


**Figure 1.** Absolute error  $E_c$  of Example 3 ( $N = 5$ ).

*Example 4.* Consider the FDE

$$D_t^{\frac{1}{3}} u(x, t) = D_x^\alpha u(x, t) + s(x, t), \quad 0 < x < 1, t > 0,$$

$$u(x, 0) = x^{\frac{7}{4}}(1 - x^{\frac{1}{2}}), \quad u(0, t) = u(1, t) = 0,$$

where the  $s(x, t)$  is a corresponding function. The exact solution is  $u(x, t) = x^{\frac{7}{4}}(1 - x^{\frac{1}{2}})(1 + t^2)$ . To highlight the differences between fractional and integer

multiwavelets bases, we present this example. We constructed bases using fractional and integer multiwavelets, and the numerical results obtained are shown in Table 3 and Figure 2. The results indicate that fractional multiwavelets bases yield more satisfactory outcomes.

**Table 3.** Results of Example 4 ( $N = 2, t = 1, \nu = 1$ ).

	$\gamma = 1$	$\gamma = \frac{1}{2}$	$\gamma = \frac{1}{3}$	$\gamma = \frac{1}{4}$
$\alpha = 3/2, d = 8$	1.74447e-03	4.15968e-04	2.48284e-05	6.66134e-16
$\alpha = 3/2, d = 16$	1.98672e-03	3.37089e-05	4.12022e-07	-
$\alpha = 3/2, d = 32$	1.01990e-03	6.54123e-06	3.22743e-08	-
$\alpha = 5/3, d = 8$	3.73272e-03	4.78743e-04	3.07157e-05	1.33227e-15
$\alpha = 5/3, d = 16$	4.84001e-03	4.70901e-05	3.88937e-07	-
$\alpha = 5/3, d = 32$	1.50908e-03	9.48701e-06	9.61464e-08	-
	$\gamma = \frac{1}{5}$			
$\alpha = 3/2, d = 8$	2.81422e-06			
$\alpha = 3/2, d = 16$	2.08974e-09			
$\alpha = 3/2, d = 32$	5.96260e-11			
$\alpha = 5/3, d = 8$	2.95762e-06			
$\alpha = 5/3, d = 16$	1.24774e-08			
$\alpha = 5/3, d = 32$	1.42617e-09			

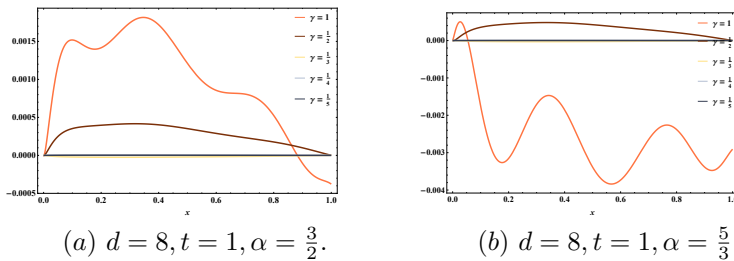


**Figure 2.** Absolute error  $E_c$  of Example 4 ( $N = 2$ ).

*Example 5.* Consider the FDE

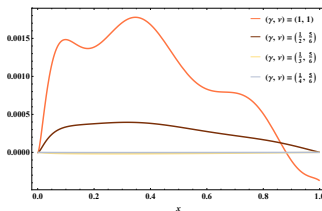
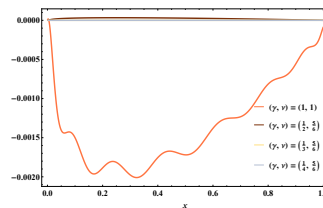
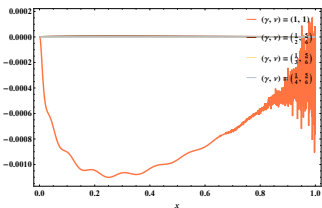
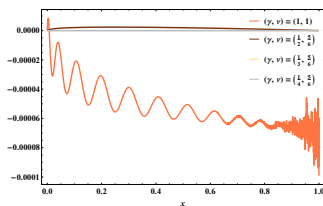
$$D_t^{\frac{1}{3}} u(x, t) = D_x^\alpha u(x, t) + s(x, t), \quad 0 < x < 1, \quad t > 0,$$

$$u(x, 0) = x^{\frac{7}{4}}(1 - x^{\frac{2}{3}}), \quad u(0, t) = u(1, t) = 0,$$

where the  $s(x, t)$  is a corresponding function. The exact solution is  $u(x, t) = x^{\frac{7}{4}}(1 - x^{\frac{2}{3}})(1 + t^{\lambda t})$ . Considering the characteristics of Example 3 and Example 4, we introduced this example to explore the effectiveness of fractional Lagrange interpolation and fractional multiwavelets. The obtained results are presented in Table 4 and Figures 3–4. These results clearly demonstrate that the application of fractional Lagrange interpolation and fractional multiwavelets offers significant advantages.

**Table 4.** Absolute error  $E_c$  of Example 4 ( $N = 2, t = 1$ ).

$(\gamma, \nu)$		(1, 1)	$(\frac{1}{2}, \frac{5}{6})$	$(\frac{1}{3}, \frac{5}{6})$
$(\alpha, \lambda_t) = (\frac{3}{2}, \frac{5}{6})$	$d = 8$	1.70813e-03	3.95039e-04	1.89809e-05
	$d = 16$	1.97624e-03	3.29807e-05	3.92364e-07
	$d = 32$	1.06528e-03	6.62115e-06	3.89960e-08
	$d = 64$	7.43866e-05	2.36446e-06	1.22804e-08
$(\gamma, \nu)$		(1, 1)	$(\frac{1}{2}, \frac{2}{3})$	$(\frac{1}{3}, \frac{2}{3})$
$(\alpha, \lambda_t) = (\frac{7}{4}, \frac{2}{3})$	$d = 8$	1.02795e-02	4.41384e-04	2.24053e-05
	$d = 16$	5.04890e-03	4.87819e-05	8.22999e-08
	$d = 32$	1.76274e-03	9.69533e-06	3.26046e-07
	$d = 64$	7.41764e-04	2.75420e-06	3.15404e-07
$(\gamma, \nu)$		$(\frac{1}{4}, \frac{5}{6})$		
$(\alpha, \lambda_t) = (\frac{3}{2}, \frac{5}{6})$	$d = 8$	2.38512e-06		
	$d = 16$	1.19795e-10		
	$d = 32$	1.07188e-10		
	$d = 64$	9.93358e-11		
$(\gamma, \nu)$		$(\frac{1}{4}, \frac{2}{3})$		
$(\alpha, \lambda_t) = (\frac{7}{4}, \frac{2}{3})$	$d = 8$	3.12543e-06		
	$d = 16$	3.06494e-09		
	$d = 32$	2.47860e-09		
	$d = 64$	1.50697e-09		

(a)  $d = 8, t = 1, \alpha = \frac{3}{2}, \lambda_t = \frac{5}{6}$ .(b)  $d = 16, t = 1, \alpha = \frac{3}{2}, \lambda_t = \frac{5}{6}$ .(c)  $d = 32, t = 1, \alpha = \frac{3}{2}, \lambda_t = \frac{5}{6}$ .(d)  $d = 64, t = 1, \alpha = \frac{3}{2}, \lambda_t = \frac{5}{6}$ .**Figure 3.** Absolute error  $E_c$  of Example 5 ( $N = 2$ ).

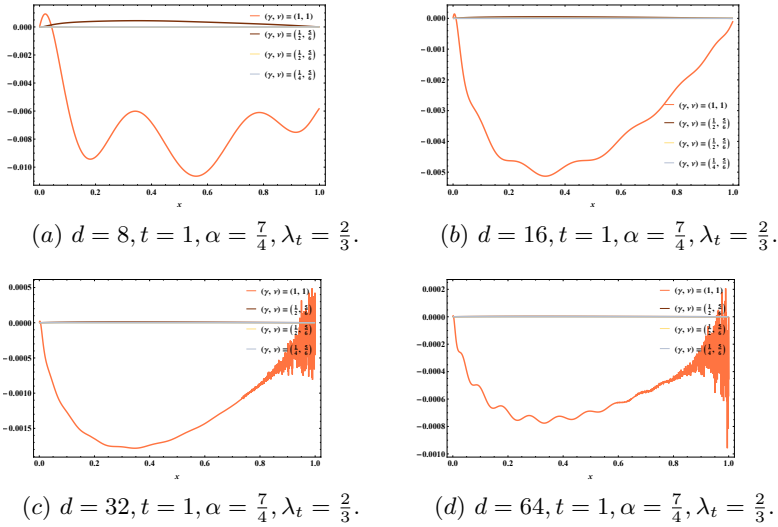


Figure 4. Absolute error  $E_c$  of Example 5 ( $N = 2$ ).

Example 6. Consider the FDE

$$D_t^{\frac{1}{3}} u(x, t) = D_x^{\frac{5}{3}} u(x, t) + s(x, t), \quad 0 < x < 1, \quad t > 0,$$

$$u(x, 0) = x^{\frac{5}{3}} \sin(3\pi x), \quad u(0, t) = u(1, t) = 0,$$

where the  $s(x, t)$  is a corresponding function. The exact solution is  $u(x, t) = x^{\frac{5}{3}} \sin(3\pi x)(1 + t^{\frac{5}{3}})$ . To demonstrate the effectiveness of fractional polynomials for both non-smooth and oscillatory solutions, we present this example. The results, showcased in Figure 5, illustrate the better effectiveness of fractional bases compared to integer bases for oscillatory solutions.

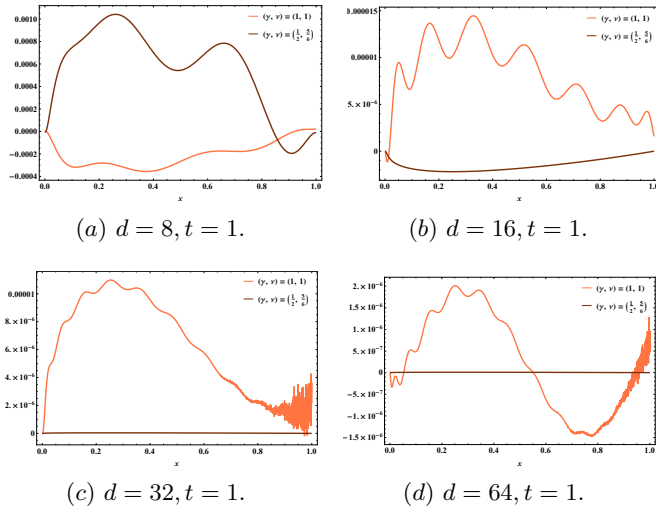


Figure 5. Absolute error  $E_c$  of Example 6 ( $N = 2$ ).

## 6 Conclusions

We employ a least residue method to address initial boundary value problems in the spatiotemporal FDE (1.1). In this approach, we obtain and analyze fractional multiwavelets. For the time variable, we use piecewise parabolic interpolation to approximate  $D_t^\beta u(x, t)$ . For the spatial variable, we utilize fractional multiwavelets as the basis to construct an approximate solution to Equations (3.5). The subsequent convergence order is analyzed. The numerical results highlight the superior performance of fractional polynomials over integer polynomials in solving differential equations with non-smooth solutions. Importantly, our method demonstrates higher accuracy compared to the Chebyshev collocation method and the finite element method. In future work, we aim to extend our method to nonlinear fractional-order systems with proportional fractional derivatives. This extension could offer new insights into systems with more complex dynamics and broaden the applicability of our approach to a wider range of real-world problems. It is worth noting that although our method faces challenges in terms of CPU time, which is an inherent consequence of using fractional polynomials, we are committed to optimizing performance and addressing this issue in future work.

## Acknowledgements

No funding has been received for this work.

## References

- [1] M. Ahmed, H.F. Ahmed and W.A. Hashem. A new operational matrices based-technique for fractional integro reaction-diffusion equation involving spatiotemporal variable-order derivative. *Int. J. Anal. Appl.*, **22**:209–209, 2024. <https://doi.org/10.28924/2291-8639-22-2024-209>.
- [2] M.P. Alam, A. Khan and P. Roul. High-resolution numerical method for the time-fractional fourth-order diffusion problems via improved quintic B-spline function. *J. Appl. Math. Comput.*, pp. 1–39, 2024. <https://doi.org/10.1007/s12190-024-02229-7>.
- [3] B. Alpert, G. Beylkin, D. Gines and L. Vozovoi. Adaptive solution of partial differential equations in multiwavelet bases. *J. Comput. Phys.*, **182**(1):149–190, 2002. <https://doi.org/10.1006/jcph.2002.7160>.
- [4] A. Baihi, A. Kajouni, K. Hilal and H. Lmou. Laplace transform method for a coupled system of (p, q)-Caputo fractional differential equations. *J. Appl. Math. Comput.*, pp. 1–20, 2024. <https://doi.org/10.1007/s12190-024-02254-6>.
- [5] S. Bu and Y. Jeon. Higher-order predictor–corrector methods for fractional Benjamin–Bona–Mahony–Burgers’ equations. *J. Appl. Math. Comput.*, pp. 1–30, 2024. <https://doi.org/10.1007/s12190-024-02223-z>.
- [6] Z. Chen, L. Wu and Y. Lin. Exact solution of a class of fractional integro-differential equations with the weakly singular kernel based on a new fractional reproducing kernel space. *Math. Meth. Appl. Sci.*, **41**(10):3841–3855, 2018. <https://doi.org/10.1002/mma.4870>.

- [7] W.H. Deng and J.S Hesthaven. Local discontinuous galerkin methods for fractional diffusion equations. *ESAIM: Math. Model. Numer. Anal.*, **47**(6):1845–1864, 2013. <https://doi.org/10.1051/m2an/2013091>.
- [8] H. Du and Z. Chen. A new method of solving the riesz fractional advection–dispersion equation with nonsmooth solution. *Appl. Math. Lett.*, **152**:109022, 2024. <https://doi.org/10.1016/j.aml.2024.109022>.
- [9] H. Du, Z. Chen and T. Yang. A stable least residue method in reproducing kernel space for solving a nonlinear fractional integro-differential equation with a weakly singular kernel. *Appl. Numer. Math.*, **157**:210–222, 2020. <https://doi.org/10.1016/j.apnum.2020.06.004>.
- [10] J. Duan and L. Jing. The solution of the time-space fractional diffusion equation based on the Chebyshev collocation method. *Indian J. Pure Appl. Math.*, pp. 1–10, 2023. <https://doi.org/10.1007/s13226-023-00495-y>.
- [11] Q. Fan, G.-Ch. Wu and H. Fu. A note on function space and boundedness of the general fractional integral in continuous time random walk. *J. Nonlinear Math. Phys.*, pp. 1–8, 2022. <https://doi.org/10.1007/s44198-021-00021-w>.
- [12] L.B Feng, P. Zhuang, F. Liu, I. Turner and Y. Gu. Finite element method for space-time fractional diffusion equation. *Numer. Algorithms.*, **72**:749–767, 2016. <https://doi.org/10.1007/s11075-015-0065-8>.
- [13] R. Gupta and S. Kumar. Space-time pseudospectral method for the variable-order space-time fractional diffusion equation. *Math. Sci.*, **18**(3):419–436, 2024. <https://doi.org/10.1007/s40096-023-00510-7>.
- [14] H. Jafari and V. Daftardar-Gejji. Solving linear and nonlinear fractional diffusion and wave equations by Adomian decomposition. *Appl. Math. Comput.*, **180**(2):488–497, 2006. <https://doi.org/10.1016/j.amc.2005.12.031>.
- [15] A.A. Kilbas, H.M. Srivastava and J.J Trujillo. *Theory and Applications of Fractional Differential Equations*, volume 204. Elsevier, Netherlands, 2006.
- [16] D. Kumar, J. Singh and S. Kumar. Analytic and approximate solutions of space-time fractional telegraph equations via Laplace transform. *Walailak J. Sci. Tech.*, **11**(8):711–728, 2014.
- [17] M. Kumar, A. Jhinga and J.T. Majithia. Solutions of time-space fractional partial differential equations using Picard’s iterative method. *J. Comput. Nonlinear Dyn.*, **19**(3):031006, 02 2024. ISSN 1555-1415. <https://doi.org/10.1115/1.4064553>.
- [18] S. Kumar, V. Gupta and D. Zeidan. An efficient collocation technique based on operational matrix of fractional-order Lagrange polynomials for solving the space-time fractional-order partial differential equations. *Appl. Numer. Math.*, **204**:249–264, 2024. ISSN 0168-9274. <https://doi.org/10.1016/j.apnum.2024.06.014>.
- [19] M. Lakestani, B.N. Saray and M. Dehghan. Numerical solution for the weakly singular fredholm integro-differential equations using legendre multiwavelets. *J. Comput. Appl. Math.*, **235**(11):3291–3303, 2011. <https://doi.org/10.1016/j.cam.2011.01.043>.
- [20] M. Li. *Theory of Fractional Engineering Vibrations*, volume 9. Walter de Gruyter GmbH & Co KG, Germany, 2021. <https://doi.org/10.1515/9783110726152>.

- [21] M.M. Meerschaert and C. Tadjeran. Finite difference approximations for fractional advection–dispersion flow equations. *J. Comput. Appl. Math.*, **172**(1):65–77, 2004. <https://doi.org/10.1016/j.cam.2004.01.033>.
- [22] M.M. Meerschaert and C. Tadjeran. Finite difference approximations for two-sided space-fractional partial differential equations. *Appl. Numer. Math.*, **56**(1):80–90, 2006. <https://doi.org/10.1016/j.apnum.2005.02.008>.
- [23] C.A. Monje, Y. Chen, B.M. Vinagre, D. Xue and V. Feliu-Batlle. *Fractional-Order Systems and Controls: Fundamentals and Applications*. Springer Science & Business Media, Germany, 2010.
- [24] P. Pandey, S. Kumar, J.F. Gómez-Aguilar and D. Baleanu. An efficient technique for solving the space-time fractional reaction-diffusion equation in porous media. *Chin. J. Phys.*, **68**:483–492, 2020. <https://doi.org/10.1016/j.cjph.2020.09.031>.
- [25] R.K. Pandey, O.P. Singh and V.K. Baranwal. An analytic algorithm for the space–time fractional advection–dispersion equation. *Comput. Phys. Commun.*, **182**(5):1134–1144, 2011. <https://doi.org/10.1016/j.cpc.2011.01.015>.
- [26] X. Qiu and X. Yue. Solving time fractional partial differential equations with variable coefficients using a spatio-temporal meshless method. *AIMS Math.*, **9**:27150–27166, 2024. <https://doi.org/10.3934/math.20241320>.
- [27] E.A. Rawashdeh. Numerical solution of fractional integro-differential equations by collocation method. *Appl. Math. Comput.*, **176**(1):1–6, 2006. <https://doi.org/10.1016/j.amc.2005.09.059>.
- [28] R. Roohi, M.H. Heydari, M. Aslami and M.R. Mahmoudi. A comprehensive numerical study of space-time fractional bioheat equation using fractional-order Legendre functions. *Eur. Phys. J. Plus.*, **133**(10):412, 2018. <https://doi.org/10.1140/epjp/i2018-12204-x>.
- [29] J. Singh, P.K. Gupta and K.N. Rai. Solution of fractional bioheat equations by finite difference method and HPM. *Math. Comput. Modell.*, **54**(9-10):2316–2325, 2011. <https://doi.org/10.1016/j.mcm.2011.05.040>.
- [30] H. Sun, A.L. Chang, W. Chen and Y. Zhang. Anomalous diffusion: fractional derivative equation models and applications in environmental flows. *Sci. Sin-Phys. Mech. Astron.*, **45**:8–22, 2015. <https://doi.org/10.1360/SSPMA2015-00313>.
- [31] C. Tadjeran and M.M. Meerschaert. A second-order accurate numerical method for the two-dimensional fractional diffusion equation. *J. Comput. Phys.*, **220**(2):813–823, 2007. <https://doi.org/10.1016/j.jcp.2006.05.030>.
- [32] P.J. Torvik and R.L. Bagley. On the appearance of the fractional derivative in the behavior of real materials. *J. Appl. Mech.*, 1984. <https://doi.org/10.1115/1.3167615>.